SENIORITY AND TRUNCATION SCHEMES FOR THE NUCLEAR CONFIGURATION INTERACTION APPROACH*

CHONG QI

Royal Institute of Technology (KTH), Alba Nova University Center, SE-10691 Stockholm, Sweden
E-mail: chongq@kth.se

Received October 30, 2014

In this contribution I would like to review a few issues on the recent developments concerning the truncation schemes for the nuclear configuration interaction shell model approach. The seniority scheme is a way to solve the pairing Hamiltonian exactly and a good starting point for shell model calculations. Physically meaningful states may also be selected based on importance truncations from a perturbation perspective.

Key words: Configuration interaction shell model, truncation, seniority.

PACS: 21.60.Gx, 23.20.-g, 21.10.-k.

1. INTRODUCTION

The nuclear interacting shell model belongs to the family of the full configuration interaction approaches. It aims to construct the wave function as a linear combination of all possible anti-symmetric Slater determinants within a so-called model space. The model space is usually defined by taking a few single-particle orbitals near the Fermi surface. The number of orbitals one can include is highly restricted due to computation limitation. Despite of this challenge, the nuclear shell model has a glorious history of success in explaining many properties of the nuclear many-body system [1]. It may be interesting to mention that such kind of configuration interaction approaches also play a decisive role in the description of other quantum many-body systems including quantum chemistry and atomic and molecular physics [2].

State-of-the-art configuration interaction algorithms are able to diagonalize matrices with dimension up to 10^{10} (10^9 with the inclusion of three-body interaction which makes the Hamiltonian matrix much more dense than that without three-body interaction). One of the major challenges of the nuclear configuration interaction calculations has been the development of practical computational approaches to handle the large-scale diagonalizing problem involved [3–11]. Whereas its application is still very much restricted since the size of the configuration space increases dramatically with the number of particles and orbitals, which soon becomes much larger

*Paper presented at the conference "Advanced many-body and statistical methods in mesoscopic systems II", September 1-5, 2014, Brasov, Romania.

than that can be treated by available diagonalizing techniques. Extensive works have been done to develop reliable truncation procedures based on perturbation methods [2, 12], Monte Carlo sampling [13–16], importance truncation [17–19] as well as density matrix renormalization group approaches [20, 21]. Brief descriptions on the different approaches can be found in Refs. [2, 17].

In this contribution I will give a brief review on some of the recent developments within the nuclear configuration interaction shell model approach and its truncation schemes (mainly works from our group due to space limitation). I will show that the seniority scheme is a way to solve the pairing Hamiltonian exactly and a good starting point for shell model calculations. I will then introduce an importance truncation approach with which bases with good angular momentum can be constructed and physically meaningful states may be selected based on from a perturbation perspective.

2. EFFECTIVE HAMILTONIAN AND THE MODEL SPACE

The basic assumption of the nuclear shell model is that the nucleons can be approximately treated as independent particles moving in a mean field that represents the average interaction between all particles. The structure properties can then be described by the correlation between valence particles around the Fermi surface [1], which was supposed to be of mainly a two-body nature. A common practice in shell model calculations is to express the effective Hamiltonians in terms of single-particle energies and two-body matrix elements as

$$H_{eff} = \sum_{\alpha} \varepsilon_{\alpha} \hat{N}_{\alpha} + \frac{1}{4} \sum_{\alpha\beta\delta\gamma JT} \langle j_{\alpha} j_{\beta} | V | j_{\gamma} j_{\delta} \rangle_{JT} A^{\dagger}_{JT;j_{\alpha}j_{\beta}} A_{JT;j_{\delta}j_{\gamma}}, \qquad (1)$$

where we have assumed isospin symmetry in the effective Hamiltonian, $\alpha = \{nljt\}$ denote the single-particle orbitals and ε_{α} stand for the corresponding single-particle energies. $\hat{N}_{\alpha} = \sum_{j_z,t_z} a^{\dagger}_{\alpha,j_z,t_z} a_{\alpha,j_z,t_z}$ is the particle number operator. $\langle j_{\alpha} j_{\beta} | V | j_{\gamma} j_{\delta} \rangle_{JT}$ are the two-body matrix elements coupled to good spin J and isospin T. A_{JT} ($A^{\dagger}_{JT}$) is the fermion pair annihilation (creation) operator. One can re-express the interaction matrix elements in the proton-neutron representation. The corresponding proton-neutron interaction matrix element is

$$\langle j_{\alpha,p} j_{\beta,n} | V | j_{\gamma,p} j_{\delta,n} \rangle_{J} = \frac{\sqrt{(1+\delta_{\alpha\beta})(1+\delta_{\gamma\delta})}}{2} \times \left[\langle j_{\alpha} j_{\beta} | V | j_{\gamma} j_{\delta} \rangle_{JT=0} + \langle j_{\alpha} j_{\beta} | V | j_{\gamma} j_{\delta} \rangle_{JT=1} \right]. \qquad (2)$$

Isospin-independence breaking interactions can also be constructed within the proton-neutron representation by considering the isospin-independence breaking effect of the nucleon-nucleon interaction and the Coulomb effect (see, *e.g.*, Refs. [22–24]).

The total energy of the state i is calculated to be

$$E_i^{\rm tot} = C + N\varepsilon_0 + \frac{N(N-1)}{2}V_1 + [T(T+1) - \frac{3}{4}N]V_0 + \langle\Psi_I|H_{eff}|\Psi_I\rangle, \quad (3)$$

where Ψ_I is the calculated shell-model wave function of the state i and I is the total angular momentum. The constant C denotes the (negative) binding energy of the core. The values of ε_0 and $V_{0,1}$ depend on the way the effective Hamiltonian is constructed. For example, in Ref. [25] we take ^{100}Sn as the inert core and include the single-particle orbitals $0g_{7/2}$, $1d_{5/2}$, $1d_{3/2}$, $2s_{1/2}$ and $0h_{11/2}$ in the model space. We assume $\varepsilon_{0g_{7/2}} = V_{0,1;0g_{7/2}^2} = 0$ and the other single-particle energies and monopole interactions are given as relative values with respect to those of the orbital $0g_{7/2}$. Thus ε_0 and $V_{0,1}$ are determined from the single-particle energy and monopole interaction of the $0g_{7/2}$ state in ^{101}Sn. It should also be mentioned that the wave function and the evolution of the effective single-particle energies within the model space are not dependent on the relative values of the monopole interactions but only on their relative values. In the other word, the excitation energy and wave function of a given state only depend on the shell model Hamiltonian H_{eff}. The relative value of the $T = 0$ and $T = 1$ monopole interaction determines the relative position of the nuclear states with different total isospin T.

One may rewrite the Hamiltonian as $H_{eff} = H_m + H_M$ where H_m and H_M denote the (diagonal) monopole and Multipole Hamiltonians, respectively. The shell model energies can be written as

$$\begin{aligned} E^{\rm SM} &= \langle\Psi_I|H|\Psi_I\rangle \\ &= \sum_\alpha \varepsilon_\alpha < \hat{N}_\alpha > + \sum_{\alpha\le\beta} V_{m;\alpha\beta} \left\langle \frac{\hat{N}_\alpha(\hat{N}_\beta - \delta_{\alpha\beta})}{1+\delta_{\alpha\beta}} \right\rangle + \langle\Psi_I|H_M|\Psi_I\rangle, \end{aligned} \quad (4)$$

where $\sum_\alpha < \hat{N}_\alpha >= N$ and

$$\sum_{\alpha\le\beta} \left\langle \frac{\hat{N}_\alpha(\hat{N}_\beta - \delta_{\alpha\beta})}{1+\delta_{\alpha\beta}} \right\rangle = \frac{N(N-1)}{2}. \quad (5)$$

The very first step for the shell model calculation is to classify the bases in terms of "partitions" or blocks which stands for a set of configurations with same definite number of particles in each orbit. The basis vectors in each partition can then be constructed within the so-called *j-j* coupled scheme [26] or the uncoupled M-scheme [27]. The mixture of basis vectors from different partitions is induced by non-diagonal two-body interaction matrix element with $\alpha \neq \gamma$ and/or $\beta \neq \delta$ in Eq. (1). The M-scheme is compatible with basic bit operations in modern computer architecture where the time-consuming calculations of coefficients of fractional parentage in *j-j* scheme can be avoided. That is the reason why most existing shell model codes

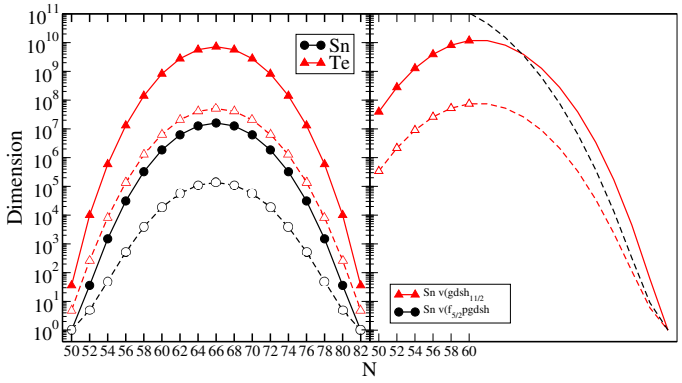

Fig. 1 – Left: Numbers of $M^\pi = 0^+$ (solid symbols) and $I^\pi = 0^+$ (open symbols) states in even-even Sn (circle) and Te (triangle) isotopes as a function of neutron numbers N in the model space $g_{7/2}dsh_{11/2}$; Right: Numbers of $M^\pi = 0^+$ (solid symbols) and $I^\pi = 0^+$ (open symbols) states in even-even Sn isotopes as a function of neutron numbers N in the model spaces $gdsh_{11/2}$ and $f_{5/2}pgdsh_{11/2}$.

are written in the M-scheme. As examples, in the left panel of Fig. 1 we plotted the total numbers of $M^\pi = 0^+$ and $I^\pi = 0^+$ states in even-even Sn and Te isotopes as a function of neutron numbers N in the model space $g_{7/2}dsh_{11/2}$ as studied in Refs. [25, 28–32].

In the M-scheme, however, only J_z and T_z are good quantum numbers. Another disadvantage is that it is difficult to apply the variety of truncation algorithms since angular momentum is not conserved. A hybrid algorithm between the M-scheme and the *j-j* coupled scheme is applied in Ref. [33] and followed in Refs. [4–6], where the symmetry of J (T) is restored through a projection procedure [34]. The dimension of the matrix can be significantly reduced through this symmetry restoration, as can be seen from Fig. 1. However, the projection process is very time-consuming and has numerical precision problems for problems involving large dimension and/or large-j shells [6].

3. SINGLE-PARTICLE TRUNCATIONS AND SENIORITY AND PAIR TRUNCATIONS

Full configuration interaction calculations can be done, with the help of supercomputers, for all nuclei shown in the left panel of Fig. 1. However, the dimension will increase dramatically and go well beyond the present computation limit if one want to expand the model space, as can be seen from the right panel of Fig. 1. The most straightforward truncation approach is to restrict the maximal/minimal numbers of particles in different orbitals, which is often referred to as single-particle truncation. This method is applied both to no-core [7] and empirical [23, 24, 28, 32, 35–37] shell model calculations. For example, in Ref. [32] we managed to study the

structure and electromagnetic transition properties of light Sn isotopes within the $gdsh_{11/2}$ model space, which involves six orbitals, by restricting the maximal number of neutrons that can be excited from the $g_{9/2}$ orbital to four.

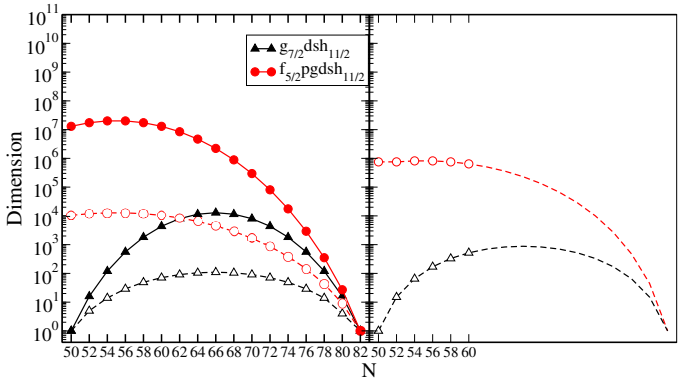

Fig. 2 – Left: Numbers of $v = 0$, $I^\pi = 0^+$ states in the jj (open) and M (solid) schemes in even-even Sn isotopes as a function of neutron numbers N in the model spaces $g_{7/2}dsh_{11/2}$ and $f_{5/2}pgdsh_{11/2}$; Right: Total numbers of partitions in even-even Sn isotopes as a function of neutron numbers N in the model spaces $g_{7/2}dsh_{11/2}$ and $f_{5/2}pgdsh_{11/2}$.

For systems involving the same kind of particles, the low-lying states can be well approximately within the seniority scheme [1]. This is related to the fact that the $T = 1$ two-body matrix elements in Eq. (1) is dominated by monopole pairing interactions with $J = 0$. The seniority quantum number is related to the number of particles that are not coupled to $J = 0$. Recent studies on the seniority coupling scheme may be found in Refs. [38–41]. One can also derive the exact solution of the pairing Hamiltonian by diagonalizing the matrix spanned by the $v = 0$, $I = 0$ states in many shells. This is applied in Ref. [42]. Such states represent only a tiny part of the total wave function, as can be seen from the comparison between Figs. 1 and 2 but are the most important components for the low-lying nuclear states. The number of $v = 0$ state is even less than the total number of partitions since there is at most one $v = 0$ state for each partition. As an illustration for the application of the seniority truncation, in the left panel of Fig. 3 we plotted the overlaps between the wave functions $|\Psi_I\rangle$ of the full Hamiltonian H and those of the pairing Hamiltonian with $J_{\max} = 0$ for the first $5/2^+$ and $7/2^+$ states in light odd-A Sn isotopes, which may be well approximated as $v = 1$ states. The empirical pairing gaps extracted from experimental and theoretical binding energies are shown in the right panel of Fig. 3 as a function of the neutron number. The overlaps of the total wave function of the first $7/2^+$ state ^{103}Sn with its leading components are calculated to be $|\langle(1d^2_{5/2})_{J=0}0g_{7/2}|\Psi\rangle_I| = 0.65$, $|\langle(0g^2_{7/2})_J0g_{7/2}|\Psi\rangle_I| = 0.62$ and $|\langle(0g_{7/2}1d_{5/2})_{J=6}1d_{5/2}|\Psi\rangle_I|$=0.57 [25].

Alternatively, one can also construct the $v = 0$ states within the "M-scheme". This is even more straightforward since the number of pairs in each $j|m|$ orbital is either zero or one. However, as can be seen from the left panel of Fig. 2, the dimension of the bases is much higher in such a scheme than that in the jj scheme. Such a scheme can also be applied to study the pairing correlation in deformed nuclei.

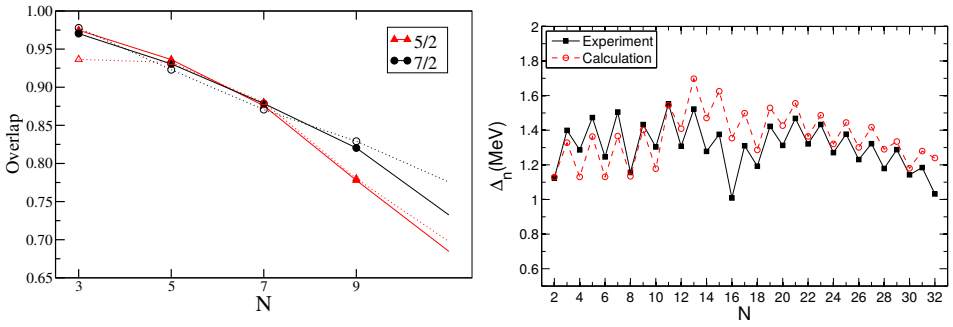

Fig. 3 – Left: Overlaps between the wave functions $|\Psi_I\rangle$ of the full Hamiltonian H and those of the full pairing Hamiltonian with $J_{\max} = 0$ (solid) and of the residual interaction with only the non-diagonal pairing matrix elements (open) for the first $5/2^+$ and $7/2^+$ states in light odd-A Sn isotopes. Right: Neutron pairing gaps in Sn isotopes extracted from the experimental and calculated binding energies.

We have also done pair-truncated shell-model calculations with collective pairs as building blocks in Refs. [43–45] for both the standard shell model and continuum shell model in the complex energy plane. The seniority coupling may be broken if both protons and neutrons are present. The effect of the maximally aligned neutron-proton pair in single-j systems was discussed in Refs. [46–49].

Recent Monte Carlo sampling calculations can be found in Refs. [13–16]. In Ref. [50] a simple Monte Carlo sampling algorithm is applied in shell model calculations in the complex energy plane. In Refs. [17–19] the importance truncation approach is applied to shell model calculations in the M-scheme. The density matrix renormalization group approach is applied to the shell model in both the jj and M schemes [20, 21]. It is seen that both the importance truncation and density matrix renormalization group approaches do not show good convergence in some cases.

4. CORRELATED BASIS TRUNCATION APPROACH

In the jj coupled scheme, vectors with good angular momentum in each partition can be expanded in M-scheme bases as

$$|\Psi_i^J\rangle = \sum_{m \le i} \mathcal{M}_{im} P^J |\alpha_m\rangle, \tag{6}$$

where P^J is the projection operator [34] and $|\alpha\rangle$ are the M-scheme bases. $\mathcal{M}$ is a lower triangle matrix. Elements of $\mathcal{M}$ can be obtained by inverting the matrix $\langle\Psi_i^J|\alpha_m\rangle$ [6].

The correlated basis truncation approach is introduced in Ref. [51]. The construction of the correlated basis is rather straight forward. First, one constructs the usual M-scheme bases. Then the correlated bases are built by diagonalizing the reduced Hamiltonian H in each partition without considering the non-diagonal matrix elements linking different partitions as

$$|\Psi_i^J\rangle(H) = \sum_m a_{im}|\alpha_m\rangle, \tag{7}$$

which also conserve the angular momentum. The Hamiltonian can then be reconstructed within the correlated basis approach, where the partial Hamiltonian H within each partition is now expressed as a diagonal matrix elements and the non-diagonal matrix elements only contains the effective interaction that connects different partitions. The total wave function can be be given as an expansion of the correlated bases by diagonalizing the corresponding Hamiltonian matrix.

Our method is similar to the angular momentum projection method [34] used in shell model codes. However, it should be emphasized that the fundamental difference between the two approaches is that our bases, which contains the most important information of the Hamiltonian within each partition, are physically meaningful as compared with the random projected basis within the projection approach [34]. One thus has the opportunity perform different truncation schemes within this approach.

It is expected that the basis vectors with lower unperturbed energy should play more important role in the low-lying states since the non-diagonal matrix elements are relatively weak in comparison to the diagonal ones. It implies that in truncating the shell model configure space one can remove those high lying basis vectors. One can evaluate the importance of a given basis vector ψ_i within a partition through a perturbation measure

$$E_g = \frac{|\langle\psi_i|H|\psi_c\rangle|}{\epsilon_i - \epsilon_c} \tag{8}$$

where ψ_c is the chosen reference state for which one may simply take the state with lowest unperturbed energy ϵ_c for the calculations of low-lying states. A similar measure is used in the importance truncation approach which is defined within the M-scheme [17]. In practice, the off-diagonal matrix element $\langle\psi_i|H|\psi_c\rangle$ (interaction between different partitions) is seldom larger than 1 MeV. Therefore the basis selecting process of ψ_c can be implicitly done by calculating the difference of unperturbed energy as

$$\epsilon_g = \epsilon_i - \epsilon_c. \tag{9}$$

An truncated model space can thus be defined by ϵ_g or E_g. If we take a sufficiently

small (large) E_g (ϵ_g), the model space will contain all the possible configurations and give the same result as a common jj-coupled scheme calculation. The reference state ψ_c may also be optimized during the iteration. The advantage of the correlated basis approach over the single-particle truncation approach is obvious since the strong correlation within each partition is not considered in the latter case.

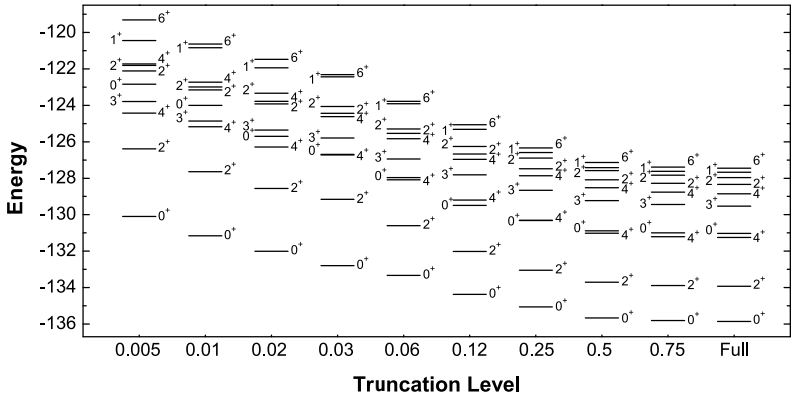

Fig. 4 – Energies of the low-lying states in ^{28}Si calculated with the correlated basis approach under different truncation levels.

As an illustration, in Fig. 4 we have performed calculations for nuclei in the sd shell within the correlated basis approach and compared with those of the standard shell model. One can see that the a very good convergence of truncation scheme is reached when the truncation model space is only one half of full model space. The convergence is even faster if we only consider the spectrum relative to the ground state. The wave function also shows a very good convergence. For the 0^+ state, the overlap is already nearly one by taking only around 2% of the total bases.

If one starts from a random M-scheme basis, the eigen vectors one obtain by diagonalizing the Hamiltonian may have different J values. A more efficient approach is to start with a basis with good angular momentum J instead which is constructed through the standard projection approach. In such a way, the eigen vectors one obtain through the Lanczos iteration approach will all have the same angular momentum.

5. SUMMARY

In this contribution we present briefly our recent works on the configuration interaction shell model calculations. The seniority scheme can serve as a way to solve the pairing Hamiltonian exactly. It is also a good starting point for practical full shell model calculations. In the correlated basis approach, the bases are taken as the eigen vectors of the partial Hamiltonian in each shell-model partition/block. The

basis wave functions thus defined conserves the angular momentum automatically. A truncation scheme can be established by taking the lowest-lying correlated bases in the different partitions. Good convergence is reached for both the energy and wave function. Large scale calculations within the correlated basis approach are under way to study the spectroscopic and transition properties of nuclei in the ^{100}Sn that cannot be reached by standard shell model calculations.

Acknowledgements. The author would like to take the opportunity to thank the organizers, particularly Prof. Delion, for giving him the opportunity to attend the conference, and L. Jiao, Z. Sun, Z. Xu, F.R. Xu, R. Wyss, R. Liotta, H. Jiang and Y.M. Zhao for collaboration. This work is supported by the Swedish Research Council (VR) under grant Nos. 621-2012-3805, and 621-2013-4323. The computations were partly performed on resources provided by the Swedish National Infrastructure for Computing (SNIC) at NSC in Linköping.

REFERENCES

1. I. Talmi, *Simple Models of Complex Nuclei* (Harwood Academic Publishers, Chur, Switzerland, 1993).
2. C. D. Sherrill and H. F. Schaefer III, Adv. Quantum Chem. **34**, 143 (1999).
3. T. Mizusaki, K. Kaneko, M. Honma, and T. Sakurai, Phys. Rev. C **82**, 024310 (2010).
4. W.D.M. Rae, Shell model code NuShellX, unpublished.
5. J. Toivanen, arXiv:nucl-th/0610028.
6. C. Qi and F.R. Xu, Chin. Phys. C **32** (S2), 112 (2008);
   C. Qi and F.R. Xu, arXiv:nucl-th/0701036 (2007).
7. J. P. Vary, P. Maris, E. Ng, C. Yang and M. Sosonkina, J. Phys.: Conference Series **180**, 012083 (2009);
   P. Maris, J. P. Vary, P. Navratil, W. E. Ormand, H. Nam, and D. J. Dean, Phys. Rev. Lett. **106**, 202502 (2011);
   P. Maris *et al.*, J. Phys.: Conference Series **403**, 012019 (2012);
   P. Maris *et al.*, J. Phys.: Conference Series **454**, 012063 (2013);
8. M. Kleinschmidt, J. Tatchen, and C. M. Marian, J. Chem. Phys. **124**, 124101 (2006).
9. E. Caurier and F. Nowacki, Acta Phys. Pol. B **30**, 705 (1999);
   http://sbgat194.in2p3.fr/~theory/antoine/
10. http://folk.uio.no/mhjensen/cp/software.html
11. Calvin W. Johnson, W. Erich Ormand, Plamen G. Krastev, Computer Physics Communications **184** (12), 2761-2774 (2013).
12. J. J. Shen, Y. M. Zhao, and A. Arima, Phys. Rev. C **85**, 064325 (2012).
13. N. Shimizu, T. Abe, Y. Tsunoda, Y. Utsuno, T. Yoshida, T. Mizusaki, M. Honma, T. Otsuka, arXiv:1207.4554 (2012);
    Y. Tsunoda, T. Otsuka, N. Shimizu, M. Honma, Y. Utsuno, arXiv:1309.5851 (2013).
14. N. Shimizu, T. Mizusaki, and K. Kaneko, Phys. Lett. B **723**, 251 (2013).
15. J. Bonnard and O. Juillet, Phys. Rev. Lett. **111**, 012502 (2013).
16. G. H. Booth, A. J. W. Thom, and A. Alavi, J. Chem. Phys. **131**, 054106 (2009).
17. R. Roth, P. Navrátil, Phy. Rev. Lett. **99**, 092501 (2007);
    R. Roth, Rhy. Rev. C **79**, 064326 (2009).

18. M. K. G. Kruse, E. D. Jurgenson, P. Navratil, B. R. Barrett, and W. E. Ormand, Phys. Rev. C **87**, 044301 (2013).
19. D. Bianco, F. Andreozzi, N. Lo Iudice, A. Porrino, and F. Knapp, Phys. Rev. C **85**, 034332 (2012).
20. T. Papenbrock and D. J. Dean, J. Phys. G Nucl. Part. Phys. **31**, S1377 (2005).
21. B. Thakur, S. Pittel, and N. Sandulescu, Phys. Rev. C **78**, 041303 (2008);
J. Dukelsky and S. Pittel, Rep. Prog. Phys. **67**, 513 (2004);
S. Pittel and N. Sandulescu, Phys. Rev. C **73**, 014301(R) (2006).
22. C. Yuan *et al.*, Phys. Rev. C **89**, 044327 (2014).
23. C. Qi, F.R. Xu, Nucl. Phys. A **800**, 47-62 (2008).
24. C. Qi, F.R. Xu, Nucl. Phys. A **814**, 48-65 (2008).
25. C. Qi and Z. X. Zu, Phys. Rev. C **86**, 044323 (2012).
26. J.B. French, E.C. Halbert, J.B. McGrory, and S.S.M. Wong, Adv. Nucl. Phys. **3**, 193 (1969).
27. R.R. Whitehead, A. Watt, B.J. Cole, and I. Morrison, Adv. Nucl. Phys. **9**, 123 (1977).
28. T. Bäck *et al.*, Phys. Rev. C **84**, 041306 (2011).
29. M.G. Procter *et al.*, Phys. Lett. B **704**, 118 (2011).
30. M.G. Procter *et al.*, Phys. Rev. C **87**, 014308 (2013).
31. M.G. Procter *et al.*, Phys. Rev. C **86**, 034308 (2012).
32. T. Bäck *et al.* Phys. Rev. C **87**, 031306 (2013).
33. A. Etchegoyen, W.D.M. Rae, N.S. Godwin, W.A. Richter, C.H. Zimmerman, B.A. Brown, W.E. Ormand, and J.S. Winfield, MSU-NSCL Report No. 524 (1985).
34. P.-O. Lodwin, Rev. Mod. Phys. **36**, 966 (1964).
35. F.G. Moradi *et al.*, Phys. Rev. C **89**(1), 014301 (2014).
36. F.G. Moradi *et al.*, Phys. Rev. C **89**, 044310 (2014).
37. C.X. Yuan, C. Qi, F.R. Xu, Nucl. Phys. A **883**, 25 (2012).
38. C. Qi *et al.*, Phys. Rev. C **82**, 014304 (2010).
39. C. Qi, Phys. Rev. C **83**, 014307 (2011).
40. C. Qi, Z.X. Xu, R.J. Liotta, Nucl. Phys. A **884–885**, 21 (2012).
41. C. Qi, Phys. Lett. B **717**, 436 (2012).
42. Z.X. Xu, C. Qi, Phys. Lett. B **724**, 247 (2013).
43. Z.X. Xu *et al.*, Nucl. Phys. A **850**, 53-68 (2011).
44. H. Jiang, C. Qi, Y. Lei, R. Liotta, R. Wyss, Y.M. Zhao, Phys. Rev. C **88** (4), 044332 (2013).
45. H. Jiang, Y. Lei, C. Qi, R. Liotta, R. Wyss, Y.M. Zhao, Phys. Rev. C **89** (1), 014320 (2014).
46. B. Cederwall *et al.*, Nature **469**, 68-71 (2011).
47. C. Qi, J. Blomqvist, T. Back, B. Cederwall, A. Johnson, R. Liotta, R. Wyss, Phys. Rev. C **84**, 021301(R) (2011).
48. Z.X. Xu, C. Qi, J. Blomqvist, R.J. Liotta, R. Wyss, Nucl. Phys. A **877**, 51 (2012).
49. C. Qi, Phys. Rev. C **81**, 034318 (2010).
50. Z.X. Xu, C. Qi, arXiv:1306.1093.
51. L.F. Jiao *et al.*, Phys. Rev. C **90**, 024306 (2014).